http://dx.doi.org/10.5935/0103-5053.20140193

J. Braz. Chem. Soc., Vol. 25, No. 11, 2063-2072, 2014.
Printed in Brazil - ©2014 Sociedade Brasileira de Química
0103 - 5053 $6.00+0.00

Article

Flame Atomic Absorption Spectrometric Determination of Pb(II) and Cd(II) in Natural Samples After Column Graphene Oxide-Based Solid Phase Extraction Using 4-Acetamidothiophenol

Mohammad R. Pourjavid,*[a] Masoud Arabieh,[a] Ali A. Sehat,[b] Mohammad Rezaee,[a] Majid H. Hosseini,[a] Seyed R. Yousefi[a] and Mohammad R. Jamali[c]

[a]*Nuclear Science & Technology Research Institute (NFCRS), P.O. Box 11365-8486, Tehran, Iran*

[b]*Department of Analytical Chemistry, Faculty of Chemistry, University College of Science, University of Tehran, P.O. Box 14155-6455, Tehran, Iran*

[c]*Department of Chemistry, Payame Noor University, P.O. Box 19395-3697, Tehran, Iran*

A determinação de chumbo e cádmio por espectrometria de absorção atômica de chama após a extração de fase sólida do óxido de grafeno (GO) utilizando o 4-acetamidotiofenol (ATP) como reagente quelante foi descrita. PM6 semi-empírico e a teoria de densidade funcional PBE foram os métodos usados na investigação do mecanismo de adsorção dos complexos em folhas de GO. Os principais fatores que influenciam a pré-concentração e determinação de analitos (pH, quantidade de ATP, tipo e concentração de eluente, fluxo e volume de amostra) foram examinados em detalhe. O efeito de íons interferentes no fator separação-pré-concentração também foi investigado. Para soluções de Pb(II) e Cd(II) 1,0 μg L^{-1}, o fator de pré-concentração chegou a 250 (em condições otimizadas). Os limites de detecção para Pb(II) e Cd(II) foram 170 e 80 ng L^{-1}, respectivamente. A validade do método proposto foi checada com materiais de referência padrão e foi aplicado com sucesso na determinacao de traços de Pb(II) e Cd(II) em amostras de água, ervas e peixe com recuperação de 99,4-103,5%.

The determination of lead and cadmium by flame atomic absorption spectrometry after solid phase extraction on graphene oxide column with use of 4-acetamidothiophenol (ATP) as chelating reagent was described. PM6 semi-empirical and PBE density functional theory methods were used to investigation of adsorption mechanism of the complexes on GO sheet. The main factors influencing the preconcentration and determination of the analytes (pH, ATP amount, eluent type and concentration, flow rate and sample volume) were examined in detail. The effect of interfering ions on the separation-preconcentration of analytes was also investigated. For Pb(II) and Cd(II) solutions of 1.0 μg L^{-1}, the preconcentration factor was as high as 250 (under the optimized conditions). The detection limits for Pb(II) and Cd(II) were 170 and 80 ng L^{-1}, respectively. The validity of the proposed method was checked with standard reference materials and it has been successfully applied for the determination of trace Pb(II) and Cd(II) in water, herbal and fish samples with the recoveries of 99.4-103.5%.

Key words: lead, cadmium, solid phase extraction, graphene oxide, acetamidothiophenol

Introduction

The importance of the determination of heavy metal ions in environmental samples can hardly be over emphasized because they have undoubtedly being a serious potential hazard to the human organism.[1] These metals are taken by human, mostly through diet, and the determination of their concentration in food and waters is very important due to their role in our body.[2] The determination of traces of heavy metal ions in environmental samples is restricted by two main difficulties: the very low concentration of heavy metal ions and the interfering effects of the matrix.[3] Flame atomic absorption spectrometric (FAAS) analysis of heavy metal ions in real samples is directly difficult, because of

*e-mail: pourjavid@gmail.com

complex formation and significant matrices.[4] In addition, some metals have low concentrations, which are near or below the limit of detection (LOD) of the instrument. To overcome these limitations, preliminary separation and preconcentration steps have been used.[5]

Due to its simplicity, solid phase extraction (SPE) is the preferred technique for the trace metal ions preconcentrations by researchers. The solid materials that have high surface area and high adsorption capacities like silica, activated carbon, Amberlite XAD or chitosan resins, polyurethane foam and nanomaterial have been widely used for this purpose.[6] An efficient solid-phase extractant should consist of a stable and insoluble porous matrix having suitable active groups (typically organic groups) that interact with heavy metal ions.

Graphene is the name given to a flat monolayer of carbon atoms tightly packed into a two-dimensional (2D) honeycomb lattice, and is the basic building block for graphitic materials of all other dimensionalities.[7] Specific properties of this interesting material have made it suitable for application in different fields. Mechanical stability, high intrinsic mobility (200,000 $cm^2\ v^{-1}\ s^{-1}$) and high theoretical specific surface area (2630 $m^2\ g^{-1}$) are some important properties of graphene.[8] Due to the high surface area of graphene; it can be used as a good adsorbent for separating of different kinds of materials. Graphene oxide (GO) has many carbonyl, carboxylic, alcoholic groups on its monolayer surface that can be used as functional groups.[9]

We have recently reported an experiment in which GO and 3-(1-methyl-1*H*-pyrrol-2-yl)-1*H*-pyrazole-5-carboxylic acid (as adsorbent and chelating reagent, respectively) were applied to separation and preconcentration of Mn and Fe ions. This experiment led to apply the proposed procedure for simultaneous determination of mentioned ions at low concentrations in various aqueous samples, such as black and green tea, spinach, human hair, blood and urine. The adsorption mechanism of titled metals complexes on GO, was investigated by using a computational chemistry approach based on PM6 semi-empirical potential energy surface (PES).[10] 2-(tert-butoxy)-*N*-(3-carbamothioylphenyl) acetamide was used for Fe, Ni, Cu and Zn separation and preconcentration, in a same system.[11] The aim of present study is to synthesize GO as a solid phase extractor and to investigate the feasibility of absorption of Pb(II) and Cd(II) on it, in the presence of the chelating agent. Synthesized material was first characterized by using transmission electron microscopy (TEM), Raman and Fourier transform infrared (FT-IR) spectroscopy. Chelates of lead and cadmium formed with 4-acetamidothiophenol (ATP) can be adsorbed on GO in column. The parameters including pH of the sample solution, amounts of ATP, sample volume, type of eluting agent and the effect of diverse ions were investigated.

Experimental

Instruments

A Shimadzu model AA-680 atomic absorption spectrometer (Japan) with a hollow cathode lamp as radiation source and a deuterium background corrector at respective wavelengths (using an air-acetylene flame) was used for metal ions determination in standard and sample solutions. All the operating parameters were those recommended by manufacturer. A Metrohm 691 pH/ion meter (Buchs, Switzerland) supplied with a combined glass-calomel electrode was used for the pH adjustments. The size and morphology of GO was observed by TEM using a CM120 microscope (Philips, Netherlands). Raman spectra of GO were prepared using a SENTERRA microscope (BRUKER, Germany). FT-IR spectra were taken on a BRUKER VECTOR 22 Spectrometer. The flow of the sample and eluent through the column was adjusted using a 10 roller peristaltic pump (Ultrateck Labs Co. Iran).

Reagents and materials

Analytical reagent-grade of acids, bases, nitrate salts of metals and other chemicals obtained from Merck (Darmstadt, Germany) were used as received. All solutions were prepared in doubly deionized water (DDW). All the plastic and glassware were cleaned by soaking in HNO_3 solution (10% v/v) and then rinsed with DDW before use. The stock standard solutions of analytes (1000 mg L^{-1}) were prepared from analytical grade of nitrate salts of the analytes. The working standard solutions were prepared by appropriate dilution stock solutions. ATP was purchased from Sigma-Aldrich.

Synthesis and characterization of GO

GO was synthesized by improved Hummers' method.[12] In this method, graphite powder (1 g, Merck) reacted with $KMnO_4$ (6 g) in a mixture of concentrated H_2SO_4/H_3PO_4 (9:1, 50 mL). Synthesized GO was characterized by TEM, Raman and FT-IR spectroscopy.

The Raman spectrum of GO includes the G peak located at ca. 1580 cm^{-1} and 2D peak at ca. 2700 cm^{-1}, caused by the in-plane optical vibrations and second-order zone boundary phonons, respectively. The D peak at ca. 1350 cm^{-1}, due to first-order zone boundary phonons, is absent from defect-free GO, but exists when the GO has defects. As can be

seen in Figure 1, the Raman spectrum result shows that GO has defects in layers (peak at ca. 1350 cm^{-1}).

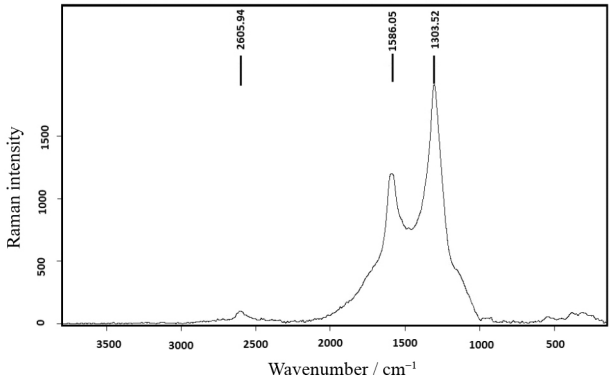

Figure 1. Raman spectra of graphene oxide.

TEM image shows that the transmittance of synthesized GO is close to that of air and for this reason the synthesized GO is likely to have a single or just a few layers. Separation of layers makes high surface area for GO.

As can be seen in Figure 2, the FT-IR spectrum of the prepared sorbent was recorded. The phenolic OH groups are indicated by the broadband peak at ca. 3500 cm^{-1}. The adsorption bands for carbonyl groups and carbon-carbon double bonds appear at 1741 cm^{-1} and 1619 cm^{-1}, respectively. The peaks from 1056 cm^{-1} to 1398 cm^{-1} identify the alcoholic and epoxy groups. Taken together, the whole FT-IR spectrum implies that GO has formed. In addition, the BET surface area shows 398.24 $m^2\ g^{-1}$ for synthesized GO.

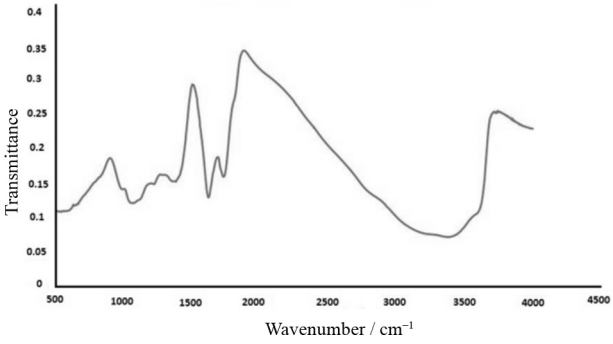

Figure 2. FT-IR spectra of graphene oxide.

Computational details

Computational chemistry has been shown to be an appropriate technique to study the interaction of different nano-carbon structures with a variety of moieties.[13] Recently, we used this method to describe the interaction between manganese (II) and iron (III) ions with GO via complexation with 3-(1-methyl-1*H*-pyrrol-2-yl)-1*H*-pyrazole-5-carboxylic acid.[10]

In the current study, to find more details on the adsorption mechanism of the titled metallic complexes on GO, we tried to improve our previous computational modeling by using both semi-empirical and density functional theory (DFT) approaches. Therefore, the geometry of all sutures including ATP, metallic complexes and GO structure were initially fully optimized at PM6 computational level. PM6 is one the most recent member of the NDDO family of semi-empirical methods and is understandably the most accurate.[14] Frequency calculations were performed to check the nature of optimized structures. DFT methods have been shown previously to reproduce experimental proprieties[15] and have been commonly used for nano structures. Consequently, for improving the calculated energies, single point energy calculations were carried out using PBE functional.[16]

PBE is a member of prominent density functional theory functional that is suggested to be appropriate functional for theoretical study on carbon-nano structures. The 6-311+G* basis set were utilized for non-metallic atoms while for Cd(II) and Pb(II), the well-known LANL2DZ effective core potential (ECP) were applied. We also considered basis set superposition error (BSSE) in adsorption energies calculations. All calculations were performed using the Gamess code.[17]

Column preparation

GO (30.0 mg) was loaded into a 100 × 8 mm glass column with upper and lower frits to avoid any loss of adsorbent. The column was preconditioned with methanol (10.0 mL) and DDW (10.0 mL), respectively.

Test procedure for SPE of Pb(II) and Cd(II)

The desired mass of GO was loaded into the column and preconditioned. The pH of the sample solution (100 mL, 10.0 μg L^{-1} of lead and cadmium) was adjusted to 6.0 using the solution of phosphate buffer and a solution of ATP (50 μL, 1.0×10^{-2} mol L^{-1}) was added. The obtained solution was passed through the column at a flow rate of 7.0 mL min^{-1}. The column was rinsed with DDW (5.0 mL) and the metal complexes retained by GO were then eluted with 2.0 mol L^{-1} HNO_3 (5.0 mL) at flow rate of 5.0 mL min^{-1}. The concentration of the metal ions in final solution was determined by FAAS.

Sample preparation

Water samples were taken from Latian and Karaj dam (Tehran, Iran). The samples were stored in 1 L glass bottles

and filtered through a filter paper (Whatman No. 40) and were acidified for storage before use. Approximately, 50 mL of each sample was treated under the general procedure. Herbal sample (5.0 g, purchased from a local market in Tehran) was digested with concentrated nitric acid until the sample solutions became clear. HCl solution was then added to ensure complete digestion. After cooling the sample to room temperature, the digested solution was diluted with DDW. Aliquots of the obtained clear solution were analyzed according to the prescribed.[18] Trout and Minnow (purchased from Tehran local fish market) were kept at −20 °C before used. After grinding the dry tissue, 0.5 g of each sample was digested by concentrated HNO_3 in Teflon beakers. To deproteinate the samples, resulted mixture was filtered into Erlenmeyer flask and then diluted with DDW.[19]

Results and Discussion

The results of computational calculations

The GO sheet can be modeled as graphene being functionalized with O-containing groups such as hydroxyl, epoxy, carboxyl, etc. on both sides and at the edges of the surface.[20] It is reasonable to consider the hydroxyl and epoxy groups as the most potent interaction sites available on GO sheet.[21] In this study, the GO surface was built in accordance with reported protocols by Guo *et al.*,[13] in which the surface includes three $C_8O_2(OH)_2$ units that can interact with other moieties. In this model, each metallic complex was parallel to the surface with the main functional groups approaching the $C_8O_2(OH)_2$ units (Figure 3). Therefore, complexes could interact with both OH and epoxy groups. The boundary effects were not applied here since the periodic boundary condition (PBC) used by calculations on the sheet are arbitrary and may affect the results qualitatively. We therefore considered a model of finite flakes GO bounded by hydrogen.

The optimized geometry of the deprotonated ligand is shown in Figure 4. A glance to the ligand structure confirms the C_{2v} symmetry point group of the molecule wherein S, O and O atoms are located in the symmetry plane of the structure.

Figure 5 shows the three accessible interaction mode in the ligand structure for metal-ligand complexation in which S, N and O atoms of the ligand may involve in complexation procedure (represented by interaction mode 1, 2 and 3, respectively).

The optimized structures of Cd(II) complexes are shown in Figure 6, while the corresponding results for Pb(II) complexes are presented in Figure 7. Approximately, the complexation procedure leads to ligand deformation in all cases. The most ligand deformation relates to one of the Pb(II) complexes in which the tail methyl group of the molecule orients toward the aromatic ring.

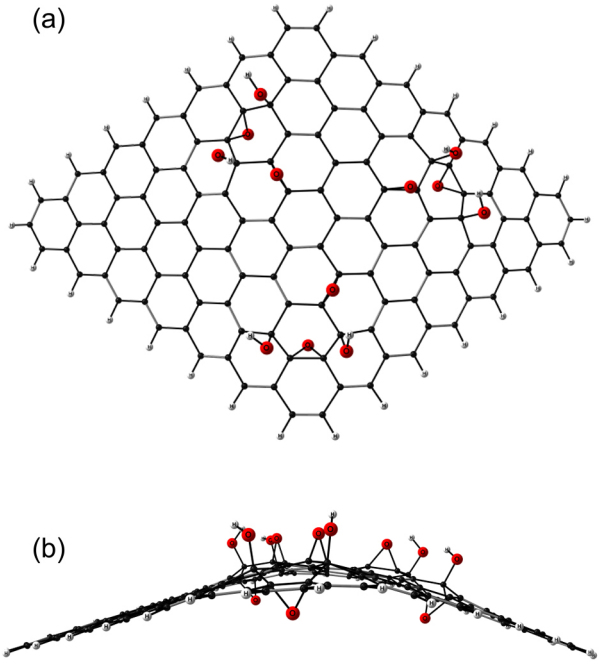

Figure 3. The optimized GO model with three $C_8O_2(OH)_2$ units on the carbon plane: (a) top view and (b) side view.

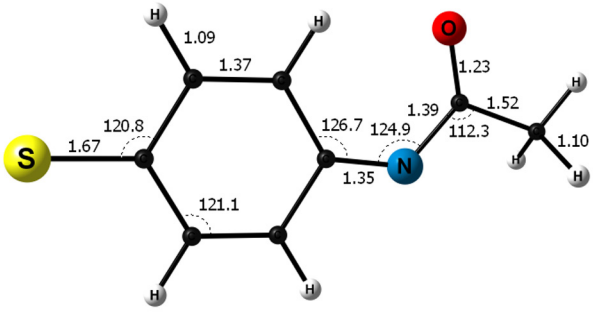

Figure 4. The optimized geometry and selected geometrical parameters of deprotonated ligand. Bond lengths are in angstrom and angles are in degree.

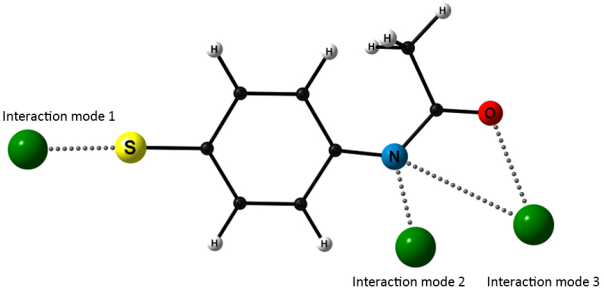

Figure 5. Different available interaction modes of ligand for complexation with metals. The green balls denotes to Cd(II) and Pb(II).

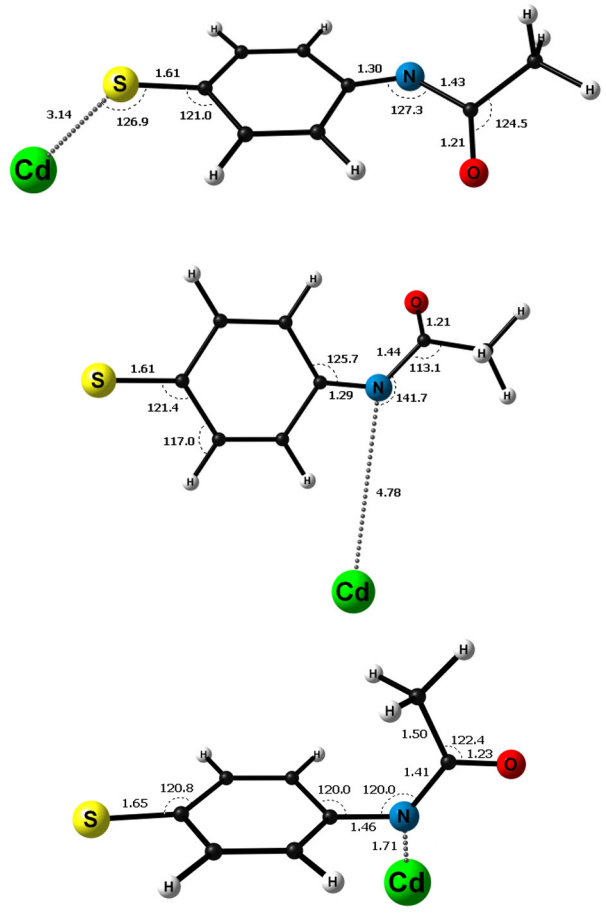

Figure 6. Optimized geometries of Cd(II) complexes at PM6 level together with selected geometrical parameters. Bonds are in angstrom and angles are in degree.

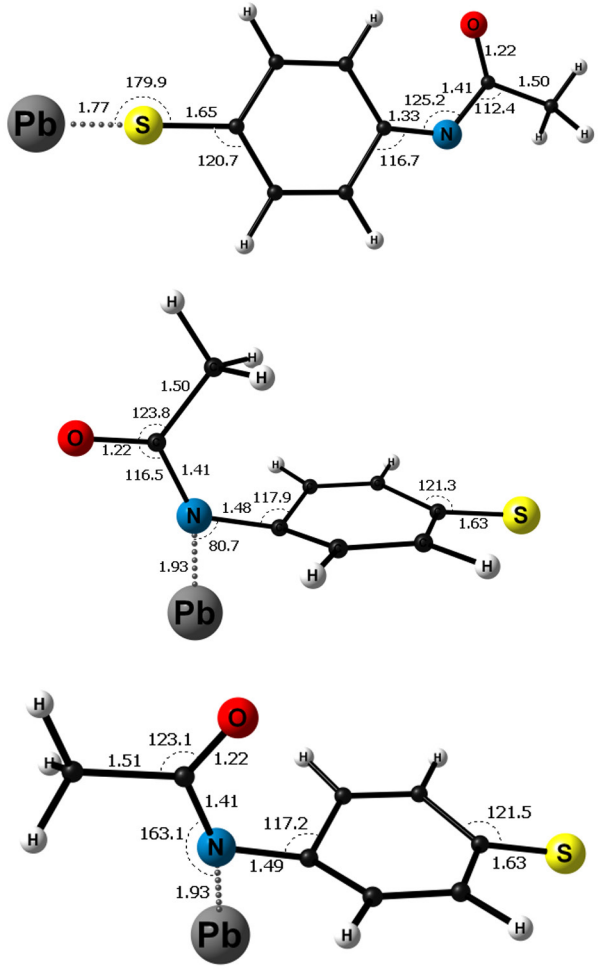

Figure 7. Optimized geometries of Pb(II) complexes at PM6 level together with selected geometrical parameters. Bonds are in angstrom and angles are in degree.

The total relative energies of complexes at two computational levels are listed in Table 1. The results show that considering the initial interaction modes, the most stable complex of Cd(II) and Pb(II) are the same at PM6 level. In other words, the most stable structures are constructed based on interaction mode 1, wherein the metals are coordinated by sulfur atom. However, improving the energies of structures at PBE/6-311+G* computational level reveals that, again, in the most stable complex of Cd(II), the sulfur atom is involved, while in Pb(II) complex, nitrogen atom contributes in coordinating the metal. Thus, the most stable complexes confirmed at DFT level are used for subsequently investigation of the adsorption of complexes on the GO sheet.

Figure 3 shows the top and side view of optimized GO at PM6 level of theory. The presence of oxygen atoms in GO structure leads to basal shape of the GO sheet in comparison to pristine graphene. This is simply because of the smoothly change in the hybridization of functionalized carbon atoms from sp^2 to sp^3.

Figure 8 shows the schematic representation of adsorbed Cd(II) and Pb(II) complexes on GO sheet, respectively. As

Table 1. Calculated relative energies of metallic complexes (at PM6 and PBE/6-311+G*//PM6 level) and adsorption energies of most stable complexes on GO sheet (at PBE/6-311+G*//PM6 level). All energies are in kcal mol^{-1}

Complex	Mode[a]	PM6	PBE[b]/PM6	E_{ads}
	1	0.0	0.0	−28.2
Cd(II)	2	0.7	289.9	–
	3	19.4	63.9	–
	3	40.1	0.0	−137.9
Pb(II)	2	42.7	5.8	–
	1	0.0	126.1	–

[a] Interaction mode of ligand; [b] PBE/6-311G*//PM6 computational level.

can be seen, the epoxy group is involved in the coordination of the metallic cation, in both cases. It seems that adsorption on GO persuade the Pb(II) to coordinate to ligand by both N and O atoms. Moreover, in the case of Pb(II), the aromatic ring re-orients toward the GO sheet which could be related to establishing π-π interaction. Such interactions play an

important role in adsorption procedures on grapheme base systems.[15] Thus it may predict that the adsorption of Pb(II) complex on GO must be more stronger than of Cd(II) complex.

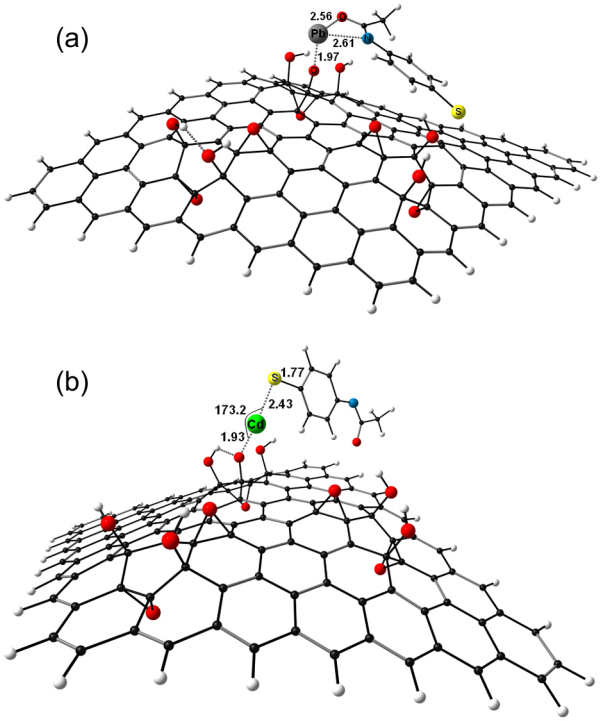

Figure 8. Calculated interaction parameters for approaching metallic complexes to graphene oxide (GO) at PM6 level. Bonds are in angstrom and angles are in degree: (a) Cd(II) complex and (b) Pb(II) complex.

It will be helpful to use adsorption energy (E_{ads}) as a quantitative scale to investigate the adsorption of complexes on GO sheet. Adsorption energy that here may consider as the intensity of interaction between titled metallic complexes and GO surface, is derived according to the following equation:

$$E_{ads} = E_{GO+Complex} - (E_{GO} + E_{Complex})$$

where E_{ads}, $E_{Complex}$ and E_{GO} represent the total energy of the adsorption system, the energy of complex and the energy of GO, respectively. A more negative E_{ads} results in a more stable adsorption system. The last column of Table 1 shows the adsorption energies of various systems. As can be seen, the adsorption of Pb(II) system leads to more negative value of E_{ads}, which is in line with previous discussion on Pb(II) complex adsorption on GO.

pH of the sample solution

The adsorption of metal complexes on GO over a range of pH was investigate. As shown in Figure 9, lead can be quantitatively recovered (≥ 96%) in the pH range 5-7.5. Quantitative recoveries were obtained in the pH range 5-7 for cadmium. The decrease in the recoveries of the lead and cadmium ions at lower pH values could be due to the competition between protons and metal ions for occupying the active sites of the sorbent.[22] At higher pH, the metal ions species may mainly hydrolyze and form $M(OH)_n$ or MOH^+. According to the results, the optimum pH was 6.0 for double-element preconcentration of the metals in question.

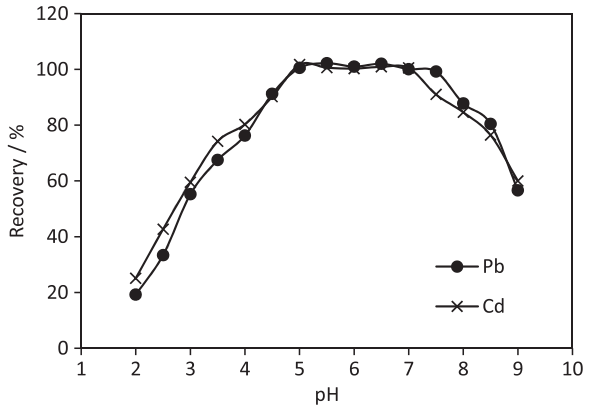

Figure 9. Effect of pH on sorption of the Pb(II) and Cd(II) ions on modified graphene, concentrations: 1.0 μg L^{-1} of Pb(II) and Cd(II).

Optimization of chelating reagent

The influences of the amount of ATP (used as the chelating agent) on the recoveries of lead and cadmium ions (keeping other parameters constant) were investigated. In the absence of ATP, the preconcentration yields of analyte ions were lower than 10%. Different volumes of 1×10^{-2} mol L^{-1} of ATP solutions were added to model solutions containing 2 μg of Pb(II) and Cd(II). The recovery values of the analyte metal ions increased and reached a constant value with the addition of 2.0-4.0 mL of ATP solution (1×10^{-2} mol L^{-1}). Because of insufficient ligand amounts in the solutions, the recoveries of analytes were not quantitative when less than 2.0 mL ATP solution was used. On the other hand, a 4.0 mL of ATP solution, the recoveries were below 95%, due to competition on the adsorption between ATP-metal chelates and excess ATP in the solution.[23,24] On this basis, 3.0 mL of ATP (1×10^{-2} mol L^{-1}) was chosen for all ensuing experiments.

Studies of eluent volume and concentration

To determine the optimal solvent for elution, various eluent solutions were used for desorption of lead and cadmium ions from GO. The results are given in Table 2. As can be seen, the analyte elements retained by the sorbent could be quantitatively desorbed with 1.5 mol L^{-1} of HNO_3 irrespective of whether they were retained on the sorbent as

their chelates with ATP or not prior to passing through the GO in the column. Therefore, 5 mL of 1.5 mol L^{-1} HNO_3 was used in the following experiments.

Table 2. Desorption of lead and cadmium ions using various eluting agents[a]

Eluent	Volume / mL	Recovery / %[b]	
		Pb	Cd
HCl (1 mol L^{-1})	2	65	60
HNO_3 (1 mol L^{-1})	2	76	74
CH_3COOH (1 mol L^{-1})	2	61	56
HNO_3 (1 mol L^{-1})	4	89	88
HNO_3 (1 mol L^{-1})	7	100	98
HNO_3 (1.5 mol L^{-1})	3	88	83
HNO_3 (2 mol L^{-1})	3	97	95
HNO_3 (2.5 mol L^{-1})	3	100	101
HNO_3 (2 mol L^{-1})	4	100	99
HNO_3 (1.5 mol L^{-1})	5	101	100
HNO_3 (1.5 mol L^{-1})	6	101	101

[a]Initial samples contained 1.0 μg L^{-1} Pb(II) and Cd(II) ions; [b]values following "±" are the standard deviation based on five replications.

Influence of flow rate

The dependence of the uptake of the metal on the flow rate was examined in the range of 3-13 mL min^{-1}. The extraction is independent of the loading flow rates in the range of 1-9 mL min^{-1}, indicating very rapid sorption kinetics. The flow rate of 9 mL min^{-1} was therefore selected during this project.

The influence of the flow rate of the eluent solution was also investigated. The results showed that when the elution flow rate varies in the range of 1-4.5 mL min^{-1}, the analytes can be recovered quantitatively (≥ 96%). Therefore, the rate of flow for the eluent solution was maintained at 4.5 mL min^{-1} in all subsequent experiments.

Effect of sample solution volume

In real samples containing very low concentration of metal ions, the maximum applicable sample volume needs to be determined by passing a given volume of solutions at the optimized flow rate. Metal ions were recovered quantitatively at the range of 25-500 mL. The elution of the studied ions from GO column occurred with recovery percentages of 97.5-100.2% in final solutions of 2 mL. At volumes higher than 500 mL, the recoveries for analytes were not quantitative. Whereas the preconcentration factor was 250, the proposed method can be used for determination of Pb(II) and Cd(II) in very low concentrations that cannot be determined directly by FAAS with sufficient accuracy.

Linear range and limit of detection

The effect of sample processing volume on analyte recovery was considered and the results show that the responses increased linearly with volume. Linear ranges were obtained for Pb(II) and Cd(II) in the concentration range of 0.35-370 and 0.20-325 μg L^{-1}, respectively ($R^2 > 0.998$). Using the optimum SPE conditions, the LOD of the method for target ions were calculated. The LOD for Pb(II) and Cd(II) was found to be 170 and 80 ng L^{-1}, respectively.

Retention capacity

To determine the adsorption capacity, sample solutions (100.0 mL) with varying concentrations of lead and cadmium concentration were adjusted to pH 6.0 with phosphate buffer and analysed under the optimum conditions. The breakthrough curves for target ions were obtained by plotting the concentration versus the mass of Pb(II) and Cd(II) adsorbed (in units of mg) *per* gram of GO. The retention capacity of GO for Pb(II) and Cd(II) ions was 17.9 and 15.3 mg g^{-1}, respectively.

Evaluation of interferences

For application of recommended SPE to real samples, effects of interference by common coexisting ions on the recovery of Pb(II) and Cd(II) were investigated under optimized conditions. In these experiments, solutions (100 mL) containing 10 μg of lead and 5 μg of cadmium and a series of interfering ions were examined. The tolerable limits of interfering ions are given in Table 3. These results indicate that some of the metal ions are tolerable up to 20-fold excess for Pb(II) and 60-fold for Cd(II).

Table 3. Effect of foreign species in the determination of 100 μg L^{-1} of Pb(II) and 50 μg L^{-1} of Cd(II)

Foreign ions	Tolerance limit / (mg L^{-1})	
	Pb	Cd
Li^+, Na^+, K^+	8000	8000
Mg^{2+}, Ca^{2+}, Ag^+	2500	3000
Mn^{2+}, Co^{2+}, Ni^{2+}, Cu^{2+}, Sn^{2+}	100	150
Fe^{2+}, Zn^{2+}, Hg^{2+}	20	60

Table 4. Determination of lead and cadmium ions in certified reference material

Certified reference material	Certified[a] / (μg kg^{-1})		Found[a] / (μg kg^{-1})	
	Pb	Cd	Pb	Cd
SRM 1640	27.89 ± 0.14	22.79 ± 0.96	26.48 ± 0.55	21.21 ± 0.63
LGC6016	196 ± 3	101 ± 2	194 ± 1	101 ± 3

[a] The values following "±" are the standard deviation based on five replications.

Applications

To evaluate the validity of the developed method, certified reference materials SRM 1640 (natural water) and LGC6016 (estuarine water) were analyzed. The certified values and the analytical results listed in Table 4 show that obtained results for the standard material are in remarkable agreement with the certified values.

The proposed method was tested successfully for the determination of Pb(II) and Cd(II) in water, herbal and fish samples. In order to validate the proposed method, recovery experiments were carried out for water samples by spiking water samples with two standard solutions of lead and cadmium before applying SPE procedure. The results in Tables 5 and 6 confirm that, despite the presence of diverse ions and species with different concentrations, Pb(II) and Cd(II) can be separated and determined with good recoveries in the range of 99.4-102.6%.

Table 5. Analysis of lead ions in different real samples

Sample	C_{added} / (μg L^{-1})	C_{found} / (μg L^{-1})	Recovery / %	RSD / %
Tap water[a]	–	N.D.[b]	–	–
	50	50.9	101.8	1.1
Mineral water[c]	–	N.D.	–	–
	50	49.7	99.4	1.3
River water (Latian dam)	–	N.D.	–	–
	50	51.2	100.4	2.5
River water (Karaj dam)	–	N.D.	–	–
	50	51.3	102.6	1.9
Lettuce	–	24.5	–	1.7
	60	86.6	103.5	2.2
Trout	–	0.9	–	0.2
	60	60.7	99.7	3.3
Minnow	–	1.7	–	0.5
	60	61.9	99.7	2.6

[a] From drinking water system of Tehran, Iran; [b] not detected; [c] Damavand mineral water.

To demonstrate that the procedure is quantitative for lead and cadmium ions determination in lettuce and fish samples, the standard addition method was used. Lettuce (5 g) and each dried fish sample (500 mg) was initially digested as described and then subjected to the proposed method. As shown in Tables 5 and 6, the recoveries were in the range from 99.7 to 103.5%, which demonstrates that this method is well operative for SPE of Pb(II) and Cd(II) in these matrices.

Table 6. Analysis of cadmium ions in different real samples

Sample	C_{added} / (μg L^{-1})	C_{found} / (μg L^{-1})	Recovery / %	RSD / %
Tap water[a]	–	N.D.[b]	–	–
	50	49.8	99.6	1.7
Mineral water[c]	–	N.D.	–	–
	50	50.4	100.8	2.4
River water (Latian dam)	–	N.D.	–	–
	50	51.0	102.0	1.9
River water (Karaj dam)	–	N.D.	–	–
	50	49.7	99.4	1.4
Lettuce	–	2.6	–	0.8
	60	62.9	100.5	1.8
Trout	–	N.D.	–	–
	60	59.9	99.8	1.6
Minnow	–	0.9	–	0.2
	60	61.3	100.7	1.9

[a] From drinking water system of Tehran, Iran; [b] not detected; [c] Damavand mineral water.

Conclusion

A synthesized GO was used as solid sorbent to separate and preconcentrate trace lead and cadmium prior to their determination by FAAS in various samples, namely water, lettuce and fish samples. Computational modeling at PM6 semi-empirical and PBE density functional theory methods showed that the adsorption of Pb(II) complex on GO sheet is different from that of Cd(II). The analytes can be extracted selectively from a sample solution at pH 6.0 even in the presence of other elements, such as alkali, alkaline earth, transition and heavy metal ions. The use of GO as the adsorbent for Pb(II) and Cd(II) ions preconcentration possessed several advantages such as simplicity, rapidity and high preconcentration factor compared with some recent reported procedures[1,18,19,23-28] in Table 7. The method presented in this study has high preconcentration

Table 7. Characteristic performance of some reported SPE of lead and cadmium ions

Sorbent	pH	Eluent	Flow rate / (mL min^{-1})	Adsorption capacity / (mg g^{-1})	PF[a]	Linear range / (μg L^{-1})	LOD[b] / (ng L^{-1})	Ref.
PVC	ca. 7	HNO_3 (3.0 mol L^{-1})	–	2.2 (Pb) 2.8 (Cd)	50	30-800 (Pb) 10-700 (Cd)	290 (Pb) 370 (Cd)	1
Nanometer alumina	7-8	HNO_3 (2.0 mol L^{-1})	3.0	16.4 (Pb) 11.1 (Cd)	250	– –	170 (Pb) 150 (Cd)	18
MWCNTs	6	HNO_3 (10% v/v)	0.5-2.0	186.4 (Pb) 178.7 (Cd)	280	3-110 (Pb) 1-100 (Cd)	1000 (Pb) 300 (Cd)	19
Chromosorb-106	9	HNO_3 in acetone (1.0 mol L^{-1})	8.0	4.56 (Pb) 2.70 (Cd)	250	240-35 × 10^4 (Pb) 350-38.5 × 10^3 (Cd)	190 (Pb) 320 (Cd)	23
MCI GEL CHD 20Y	8	HNO_3 (1.0 mol L^{-1})	10.0	18.0 (Pb) 12.0 (Cd)	300	0.012-150 (Pb) 0.010-110 (Cd)	1.3 (Pb) 1.2 (Cd)	24
MnO_2/CNTs	6	HNO_3 (1.5 mol L^{-1})	1.0	6.7 (Pb) 9.1 (Cd)	100	– –	4400 (Pb) 1500 (Cd)	25
Amberlit XAD-2010	6	HNO_3 in acetone (1.0 mol L^{-1})	10.0	5.7 (Pb) 6.0 (Cd)	100	130-8000 (Pb) 30-1100 (Cd)	260 (Pb) 80 (Cd)	26
Solid sulfur	8	HNO_3 (1.0 mol L^{-1})	1.0	0.0156 (Pb) 0.0034 (Cd)	250	10-300 (Pb) 1-20 (Cd)	3200 (Pb) 200 (Cd)	27
Graphene	6	HNO_3 (2.0 mol L^{-1})	2.0	16.6 (Pb)	125 (Pb)	10-600 (Pb)	610 (Pb)	28
Graphene oxide	6	HNO_3 (1.5 mol L^{-1})	9.0	17.9 (Pb) 15.3 (Cd)	250	0.35-370 (Pb) 0.20-325 (Cd)	170 (Pb) 80 (Cd)	Current work

[a] Preconcentration factor; [b] limit of detection.

factor (250). In short, the developed method is suitable for preconcentration and separation of trace metal ions in real samples.

References

1. Marahel, F.; Ghaedi, M.; Shokrollahi, A.; Montazerozohori, M.; Davoodi, S.; *Chemosphere* **2009**, *74*, 583.
2. Marahel, F.; Ghaedi, M.; Montazerozohori, M.; Nejati Biyareh, M.; Nasiri Kokhdan, S.; Soylak, M.; *Food Chem. Toxicol.* **2011**, *49*, 208.
3. Ensafi, A. A.; Zendegi Shiraz, A.; *J. Braz. Chem. Soc.* **2008**, *1*, 11; Pohl, P.; Stecka, H.; Greda, K.; Jamroz, P.; *J. Braz. Chem. Soc.* **2012**, *6*, 1098.
4. Yavuz, E.; Tokalıoğlu, Ş.; Şahan, S.; *J. Braz. Chem. Soc.* **2013**, *5*, 736; Pohl, P.; Stecka, H.; Jamroz, P.; *J. Braz. Chem. Soc.* **2012**, *4*, 710; Santos, D. S. S.; Korn, M. G. A.; Guida, M. A. B.; Santos, G. L.; Lemos, V. A.; Teixeira, L. S. G.; *J. Braz. Chem. Soc.* **2011**, *3*, 552.
5. Prasad, K.; Gopikrishna, P.; Kala, R.; Rao, T. P.; Naidu, G. R. K.; *Talanta* **2006**, *69*, 938.
6. Sant'Ana, O. D.; Jesuino, L. S.; Cassella, R. J.; Carvalho, M. S.; Santelli, R. E.; *J. Braz. Chem. Soc.* **2003**, *5*, 728; Lemos, V. A.; David, G. T.; Santos, L. N.; *J. Braz. Chem. Soc.* **2006**, *4*, 697; Pilau, E. J.; Silva, R. G. C.; Jardim, I. C. F. S.; Augusto, F.; *J. Braz. Chem. Soc.* **2008**, *6*, 1136; Tuzen, M.; Saygi, K. O.; Soylak, M.; *J. Hazard. Mater.* **2008**, *152*, 632; Duran, A.; Tuzen, M.; Soylak, M.; *J. Hazard. Mater.* **2009**, *169*, 466; Liu, Y.; Cao, X.; Le, Z.; Luo, M.; Xu, W.; Huang, G.; *J. Braz. Chem. Soc.* **2010**, *3*, 533.
7. Geim, A. K.; Novoselov, K. S.; *Nat. Mater.* **2007**, *6*, 183.
8. Bolotin, K. I.; Sikes, K. J.; Jiang, Z.; Klima, M.; Fudenberg, G.; Hone, J.; Kim, P.; Stormer, H. L.; *Solid State Commun.* **2008**, *146*, 351; Morozov, S. V.; Novoselov, K. S.; Katsnelson, M. I.; Schedin, F.; Elias, D. C.; Jaszczak, J. A.; Geim, K.; *Phys. Rev. Lett.* **2008**, *100*, 016602.
9. Zhu, Y.; Murali, S.; Cai, W.; Li, X.; Suk, J. W.; Potts, J. R.; Ruoff, R. S.; *Adv. Mater.* **2010**, *22*, 3906.
10. Pourjavid, M. R.; Akbari Sehat, A.; Arabieh, M.; Yousefi, S. R.; Haji Hosseini, M.; Rezaee, M.; *Mater. Sci. Eng., C* **2013**, *35*, 370.
11. Pourjavid, M. R.; Akbari Sehat, A.; Haji Hosseini, M.; Rezaee, M.; Arabieh, M.; Yousefi, S. R.; Jamali, M. R.; *Chin. Chem. Lett.* **2014**, *25*, 791.
12. Marcano, D. C.; Kosynkin, D. V.; Berlin, J. M.; Sinitskil, A.; Sun, Z.; Slesarev, A.; Alemany, L. B.; Lu, W.; Tour, J. M.; *ACS Nano* **2010**, *4*, 4806.
13. Guo, Y.; Lu, X.; Weng, J.; Leng, Y.; *J. Phys. Chem. C* **2013**, *117*, 5708; Vanin, M.; Mortensen, J. J.; Kelkkanen, A. K.; Garcia-Lastra, J. M.; Thygesen, K. S.; Jacobsen, K. W.; *Phys. Rev. B: Condens. Matter Mater. Phys.* **2010**, *81*, 081408; Ao, Z.; Jiang, M. Q.; *Open Nanosci. J.* **2009**, *3*, 34; Krasheninnikov,

A. V.; Nieminen, R. M.; *Theor. Chem. Acc.* **2011**, *129*, 625; Yang, J. W.; Chen, X. R.; Song, B.; *J. Phys. Chem. C* **2013**, *117*, 8475; Lim, D. H.; Negreira, A. S.; Wilcox, J.; *J. Phys. Chem. C* **2011**, *115*, 8961.

14. Stewart, J. J. P.; *J. Mol. Model.* **2007**, *13*, 1173.
15. Rajesh, C.; Majumder, C.; Mizuseki, H.; Kawazoe, Y.; *J. Chem. Phys.* **2009**, *130*, 124911; Cazorla, C.; Shevlin, S. A.; Guo, Z. X.; *Phys. Rev. B: Condens. Matter Mater. Phys.* **2010**, *82*, 155454; Bagheri, Z.; Ahmadi Peyghan, A.; *Theor. Chem.* **2013**, *1008*, 20.
16. Perdew, J. P.; Burke, K.; Ernzerhof, M.; *Phys. Rev. Lett.* **1996**, *77*, 3865.
17. Schmidt, M. W.; Baldridge, K. K.; Boatz, J. A.; Elbert, S. T.; Gordon, M. S.; Jensen, J. H.; Koseki, S.; Matsunaga, N.; Nguyen, K. A.; Su, S.; Windus, T. L.; Dupuis, M.; Montgomery, J. A.; *J. Comput. Chem.* **1993**, *14*, 1347.
18. Ezoddin, M.; Shemirani, F.; Abdi, K.; Khosravi Saghezchi, M.; Jamali, M. R.; *J. Hazard. Mater.* **2010**, *178*, 900.
19. Nabid, M. R.; Sedghi, R.; Bagheri, A.; Behbahani, M.; Taghizadeh, M.; Abdi Oskooie, H.; Heravi, M. M.; *J. Hazard. Mater.* **2012**, *203-204*, 93.
20. He, H.; Klinowski, J.; Forster, M.; Lerf, A.; *Chem. Phys. Lett.* **1998**, *278*, 53; Kuila, T.; Bose, S.; Khanra, P.; Mishra, A. K.; Kim, N. H.; Lee, J. H.; *Carbon* **2012**, *50*, 914.
21. Gao, W.; Alemany, L. B.; Ci, L.; Ajayan, P. M.; *Nat. Chem.* **2009**, *1*, 403.
22. Murat Kalfa, O.; Yalçınkaya, Ö.; Rehber Türker, A.; *J. Hazard. Mater.* **2009**, *166*, 455.
23. Tuzen, M.; Parlar, K.; Soylak, M.; *J. Hazard. Mater.* **2005**, *121*, 79.
24. Yang, G.; Fen, W.; Lei, C.; Xiao, W.; Sun, H.; *J. Hazard. Mater.* **2009**, *162*, 44.
25. Yang, B.; Gong, Q.; Zhao, L.; Sun, H.; Ren, N.; Qin, J.; Xu, J.; Yang, H.; *Desalination* **2011**, *278*, 65.
26. Duran, C.; Gundogdu, A.; Numan Bulut, V.; Soylak, M.; Elci, L.; Basri Sentürk, H.; Tüfekci, M.; *J. Hazard. Mater.* **2007**, *146*, 347.
27. Parham, H.; Pourreza, N.; Rahbar, N.; *J. Hazard. Mater.* **2009**, *163*, 588.
28. Wang, Y.; Gao, S.; Zang, X.; Li, J.; Ma, J.; *Anal. Chim. Acta* **2012**, *716*, 112.

Submitted on: June 8, 2014
Published online: August 19, 2014